Compressed Antisolvent Precipitation and Photopolymerization To Form Highly Cross-Linked Polymer Particles

ARTICLE *in* MACROMOLECULES · APRIL 2002

Impact Factor: 5.8 · DOI: 10.1021/ma011955k

3 AUTHORS, INCLUDING:

Kristi Anseth
University of Colorado Boulder
355 PUBLICATIONS **20,403** CITATIONS

Article

Compressed Antisolvent Precipitation and Photopolymerization To Form Highly Cross-Linked Polymer Particles

Jennifer L. Owens, Kristi S. Anseth, and Theodore W. Randolph

Macromolecules, **2002**, 35 (11), 4289-4296• DOI: 10.1021/ma011955k • Publication Date (Web): 19 April 2002

Compressed Antisolvent Precipitation and Photopolymerization To Form Highly Cross-Linked Polymer Particles

Jennifer L. Owens,[†,‡] Kristi S. Anseth,[†,‡,§] and Theodore W. Randolph*[,†,‡]

Department of Chemical Engineering, Center for Pharmaceutical Biotechnology, and Howard Hughes Medical Institute, University of Colorado, Boulder, Colorado 80309-0424

Received November 9, 2001; Revised Manuscript Received February 28, 2002

ABSTRACT: We present a novel antisolvent processing technique by simultaneous compressed antisolvent precipitation and photopolymerization for forming cross-linked polymer microparticles. In this process, an organic solvent dissolves monomer and polymerization photoinitiators to form a homogeneous solution. Photopolymerization and microparticle formation occur when the homogeneous solution is sprayed into a compressed antisolvent while being simultaneously exposed to initiating light. High miscibility of the solvent in the supercritical antisolvent allows for its quick extraction from the polymerizing phase, leaving progressively higher concentrations of monomer. The high monomer concentration combined with photoinitiated polymerization facilitates rapid reaction rates and ultimately results in polymer precipitation. Particle size and morphology are adjustable by changing the processing conditions, as simultaneous polymerization and solvent extraction result in microparticles with a wide range of diameters.

Introduction

Polymer microparticles are produced using an assortment of methods, and new techniques are continuously being developed. Polymer microparticles are used for a wide variety of applications, ranging from industrial to medical purposes.[1−8] Many of these applications, especially those for medical use, require particles with low residual solvent levels, high additive encapsulation efficiencies, low processing temperatures, controlled particle size and morphology, and efficient bulk production capability.[9]

A common conventional method for forming polymer microparticles is solvent emulsion evaporation (SEE). This process uses a double emulsion method to precipitate particles containing drugs. Although successful on a bench scale,[10−16] the process is difficult to scale up, uses large quantities of environmentally unfriendly solvents, and is challenging to operate aseptically. Furthermore, because SEE requires dissolving the polymer in a solvent, it is unsuitable for processing insoluble, cross-linked polymers.

Another conventional method for forming polymeric microparticles is emulsion polymerization.[10,17−21] This process involves combinations of solvents, emulsifiers, and surfactants where dispersed droplets of monomer polymerize in a continuous solvent phase. Emulsion polymerization can be used to make microparticles of highly cross-linked polymers. Drawbacks of the process include the high processing temperatures necessary for thermal polymerization, the use of large quantities of solvents, and difficulties in incorporating additives in the polymer matrix.

Supercritical fluid processing (SFP) can be used to overcome some of the disadvantages of conventional methods of microparticle production.[22] Carbon dioxide is a particularly attractive supercritical fluid because it is environmentally benign and inexpensive and allows processing at moderate temperatures (e.g., 35 °C). Three current methods for producing polymer particles by SFP are rapid expansion of supercritical solution (RESS), precipitation by a compressed antisolvent (PCA), and supercritical fluid emulsion polymerization. RESS entails dissolving a solute into a supercritical fluid, followed by rapid precipitation upon subsequent depressurization of the mixture to atmospheric conditions. The resulting precipitate is comprised of microparticles on the order of 4−25 μm.[23,24] The RESS process suffers from two main drawbacks, especially when applied to polymer processing. First, polymer solubilities in supercritical carbon dioxide are typically very low.[25] For example, the equilibrium solubility of 5500 molecular weight poly(L-lactic acid) in CO_2 at 250 bar and 55 °C is only 0.01 wt %.[24] Second, the process inherently requires large changes in pressure, making the economics unfavorable.

Unlike the RESS process, PCA involves dissolving a solute into a liquid solvent prior to spraying the mixture into a compressed antisolvent. The antisolvent properties facilitate extraction of the solvent leading to solute precipitation.[26−29] Process variables such as temperature, pressure, polymer concentration, and spray characteristics can be manipulated to alter the morphology of the resulting precipitate.[27] However, conventional CO_2-based PCA processes to make polymeric microparticles are limited in several aspects. PCA requires that starting materials be dissolved in a solvent, so cross-linked polymers are impossible to process. Furthermore, because supercritical CO_2 is an effective plasticizer,[26,30] discrete microparticles can only be formed if the polymer exhibits sufficient crystallinity[30] or if the temperature is maintained below the polymer's glass transition temperature (T_g) at given solution conditions (i.e., pressure and cosolvent concentrations).[26] In particular, the relatively low T_gs of many linear polymers severely restrict the applicability of conventional PCA for microparticle manufacturing.[26,30]

Alternatively, polymer particles can be formed from polymerizations in carbon dioxide[31−33] which involves

† Department of Chemical Engineering.
‡ Center for Pharmaceutical Biotechnology.
§ Howard Hughes Medical Institute.
* Corresponding author: e-mail Theodore.Randolph@colorado.edu; Fax (303) 492-4341.

10.1021/ma011955k CCC: $22.00
Published on Web 04/19/2002

monomer, a thermal initiator, and a fluorinated polymer surfactant introduced into a high-pressure cell where the contents are thoroughly mixed, and the temperature is increased to induce thermal polymerization. Polymerizations conducted in supercritical carbon dioxide offer advantages of reduced drying times and superior particle size control over traditional solution-based methods. In addition, production of particles with controlled size and physical properties made of high-demand polymers such as polystyrene,[34] poly(acrylic acid),[35] poly(methyl methacrylate),[36,37] and poly(vinyl acetate)[38] is possible with concurrent reduction of both the overall energy necessary for synthesis and process waste. After reaction (1−4 h) the cell is cooled and depressurized, and the polymer product is collected. Unfortunately, there are several drawbacks to this process including the need for expensive fluorinated surfactants, elevated temperatures that may preclude encapsulation of therapeutic agents, and requirements for further separation of process waste.

Photopolymerization of aerosols can produce relatively monodisperse, smooth particles.[39,40] A monomer and photoinitiator solution, with or without solvent, is aerosolized into air and illuminated with light of an appropriate wavelength in order to photopolymerize the particles. However, this process suffers from poor yield, likely due to sluggish solvent evaporation and insufficient polymerization.

Herein, we propose a new technique that uses supercritical CO_2 to produce highly cross-linked polymeric microparticles. In this technique, which we term compressed antisolvent precipitation and photopolymerization (CAPP), reactive multifunctional monomers and photoinitiators dissolved in a suitable diluent are sprayed into supercritical CO_2, where photopolymerization is initiated in situ to produce cross-linked polymer particles. While such a process retains the advantages of other supercritical CO_2 processes (environmentally friendly, inexpensive solvent, low-temperature processing, etc.), it also requires only minimal amounts of organic solvents and allows flexibility in their choice. Manipulation of initiation conditions (i.e., light intensity, initiator type, initiator concentration) as well as monomer choice (i.e., functional group type and concentration) affords control over the particle size and morphology, without the use of expensive surfactants. For applications requiring biodegradable microparticles, the wide choice of available multifunctional monomer chemistries[41−43] provides a means for tailoring degradation and resultant additive release rates over a wide range of time scales. In this work, we show the feasibility of such a process and demonstrate advantages in terms of flexibility in solvent and monomer choice as well as control of particle morphology.

Specifically, we prepared cross-linked polymeric microparticles by atomizing homogeneous solutions containing organic solvent, monomer, and photoinitiator into a high-pressure chamber containing compressed CO_2 while simultaneously illuminating the chamber with high intensity ultraviolet light. We studied diacrylated poly(ethylene glycol) (PEG) monomers that react to form highly cross-linked polymer networks. We measured the reaction characteristics of the poly(ethylene glycol) monomer to help elucidate the polymerization behavior in the CAPP system. The effects of changing process and formulation variables (i.e., light intensity and initiator concentration) on the morphology and particle size of the resulting cross-linked microparticles were investigated.

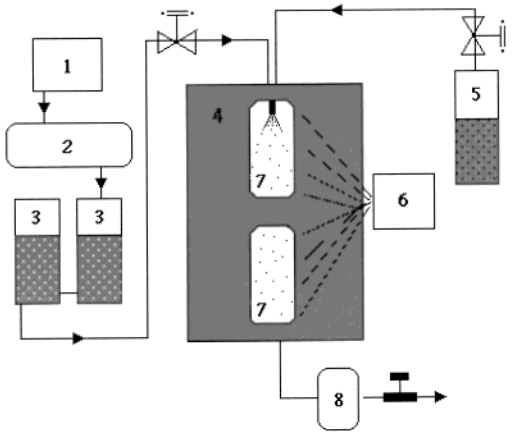

Figure 1. Schematic of CAPP system: 1, antisolvent supply; 2, oxygen scrubber; 3, antisolvent delivery pumps; 4, chamber; 5, solvent/monomer supply; 6, UV light source; 7, borosilicate windows; 8, 0.2 μm filter.

Experimental Section

Materials. The multifunctional monomer PEG1000 diacrylate (PEG1KDA, Dajack) was used as received. Methylene chloride (Fisher) was used as the solvent and dried overnight using molecular sieves (Aldrich). The photoinitiator 2,2-dimethoxy-2-phenylacetophenone (DMPA, Ciba Geigy) was employed in conjunction with a high-powered ultraviolet light source (Novacure with 100 W Hg arc lamp, EFOS, Mississaugua, Ontario, Canada) to initiate polymerization.

Particle Production. Figure 1 shows a schematic of the experimental apparatus, which is modified from the PCA system previously developed for precipitating linear polymers.[26,29,44−46] Medical grade CO_2 (US Welding) {1} was deoxygenated with an O_2 scrubber (Labclear, Oakland, CA) {2} and transferred to two compressed gas pumps (ISCO) {3} at a temperature of −10 °C. An additional ISCO pump contained the reactant solution {5}. The high-pressure chamber {4} was pressurized with deoxygenated CO_2 and allowed to equilibrate to 8.5 MPa at 35 °C. Reactant solutions for the photopolymerization CAPP process were prepared by dissolving 25 wt % PEG1000 diacrylate in dry methylene chloride and 0.1−4 wt % (relative to monomer) of the photoinitiator, DMPA. The monomer−solvent−initiator solution was then pressurized to 8.5 MPa by a third pump. The solution was atomized using a 100 μm quartz capillary tube (Alltech) into the chamber {4} at a constant flow rate (1 mL/min) through the capillary nozzle. Concurrently, the CO_2 flowed at a constant rate of 25 mL/min through a heat exchanger (at 37 °C) followed by a $^1/_4$ in. stainless steel tube into the high-pressure chamber. The quartz capillary tube was positioned in the center of the $^1/_4$ in. tube while the CO_2 flowed in the annular region. Two high-powered light sources (1−8 W/cm^2) with ultraviolet filters (320−500 nm band-pass) and fiber-optic liquid light guides supplied the light to initiate the photopolymerization below the nozzle. A 5 cm Light Line (EFOS) was used to spread the beam from one of the light guides to give a longer exposure path in the chamber as the particles passed by the illuminated windows.

Initiator molecules in the monomer/initiator particles (the solvent is rapidly extracted by the CO_2) dissociate to form radicals upon exposure to the initiating light {6} through the borosilicate windows {7}. These radicals propagate through double bonds on the multifunctional monomers to form cross-linked particles. After spraying and polymerization, the system was "washed" with several volumes of CO_2 before slow depressurization (∼30 min) at the operating temperature. After depressurization, the particle product was collected from both

the inside of the high-pressure chamber {4} and a 0.2 μm filter {8} (Millipore) at the outlet.

Particle Size and Morphology. The resulting particles were attached to aluminum stubs using colloidal graphite and coated with a thin layer of gold before being examined using a scanning electron microscope (SEM, ISI SX30) to determine their size and morphology. A TSI Aerosizer (TSI 3325, St. Paul, MN) equipped with a dry powder particle disperser (TSI Aerodisperser 3230) was used to determine the particle size distribution. Samples of roughly 0.05 g were dispersed in the aerosizer and measured with the fine particle (0.1−200 μm) power setting.

Fourier Transform (FTIR) and Real-Time (RTIR) Infrared Spectroscopy. The double-bond conversion was examined with a Nicolet FTIR spectrophotometer (model 750 Magna series II FTIR, Nicolet, Madison, WI) equipped with a MCT/B−KBr detector beam splitter combination with a resolution of 4 cm^{-1}. A horizontal transmission accessory enabled mounting of the samples horizontally so that thicker films in the near-IR region could be measured without suffering from the problems associated with gravity acting on vertically mounted liquid samples.[47] Spectra were measured in both the mid-IR (800−3000 cm^{-1}) and near-IR (5000−7000 cm^{-1}) ranges where the absorptions due to carbon−carbon double bonds were measured at 1635 and 6160 cm^{-1}, respectively.

The RTIR technique is described elsewhere[48] and was used to monitor the photopolymerization of the PEG1KDA monomer as a function of solvent concentration and initiation rate. Fractional conversion was calculated by subtracting the area of the carbon−carbon double bond peak of the reacted sample from that of the unreacted monomer and then dividing by the peak area of the unreacted monomer. For the processed particles and mechanical creep samples, conversion was quantified by ratioing the area of the carbon−carbon double-bond doublet peak at 1635 cm^{-1} to the area of the internal carbonyl reference peak at 1725 cm^{-1} (which does not change during the polymerization) and compared to that same ratio of the unreacted monomer.

Gel Point Measurements. FTIR spectra were recorded to find the conversion as a function of polymerization time, and the data were combined with macroscopic observations of the polymerizing mixture to identify gel point conversions for various monomer solutions. The gel point was defined functionally as the point at which the sample in the cuvette was no longer a liquid and ceased to flow. Solutions containing 15, 25, and 40 wt % PEG1KDA dissolved in dry methylene chloride and combined with 2 wt % DMPA (based on the monomer concentration) were used for this study. Solutions were placed in 1 cm quartz cuvettes and capped with little headspace to minimize solvent evaporation. Cuvettes were placed in the FTIR sample chamber and illuminated from above for short periods (10−15 s) of time with 10 mW/cm^2 of 365 nm ultraviolet light (EFOS, Ultracure). After each illumination time, a spectrum was collected (64 scans averaged) to determine the fractional conversion, and the samples were examined qualitatively to determine whether the gel point had been reached.

Polymerization Rate as a Function of Light Intensity. Solutions of 50 wt % PEG1KDA and 2 wt % DMPA (relative to monomer) were dissolved in dry methylene chloride. Samples sandwiched between KBr crystals were placed in the FTIR sample chamber and were illuminated for the duration of the reaction with 1, 10, and 20 mW/cm^2 of 365 nm ultraviolet light (EFOS, Ultracure). The light intensity was measured with a Cole Parmer radiometer. The reaction was deemed finished when no further changes in the absorbance intensity of the carbon−carbon double bond peak were observed. The conversion was calculated using peak area analysis as described above.

FTIR Analysis of Microparticles. Polymerization of the multifunctional PEG1KDA monomer during the CAPP particle processing was confirmed by FTIR analysis of the double-bond conversion of the particles and compared to the PEG1KDA monomer. Particles were combined with mineral oil and crushed uniformly using a mortar and pestle to create a smooth paste of oil and crushed particles. A spectrum (64 scans averaged) was acquired in the mid-IR region of the resulting paste sandwiched between two KBr crystals. The same technique was employed to make samples of the PEG1KDA monomer, and the fractional conversion of the particles was quantified as described previously.

Mechanical Creep Studies. Mechanical creep studies were performed to identify the critical conversion required to produce gelled polymer particles that would not agglomerate during the CAPP process. Creep studies were performed on standard tensile samples[30] with dimensions of 38.1 mm by 15.9 mm. Pure PEG1KDA was combined with 2% DMPA, and the solution was heated to its melting point and poured into a stainless steel mold. Glass slides sandwiched the macromer in the mold and were held in place using binder clips. Samples were polymerized in a conveyer belt UV processor system (RPC Industries) with lamps that emit throughout the UV and visible range. Fractional conversion in the samples was varied using light intensities between 0.35 and 0.8 W/cm^2 and exposure times from 5 to 20 s. Samples were removed from the mold, and midrange FTIR spectra (64 scans averaged) were collected to determine the fractional conversion as described previously. The samples were then suspended from one end by a thick string in the high-pressure chamber, which was filled with CO_2 to various pressures. The creep stress was provided by gravity acting on the suspended samples.

Initially, CO_2 at 5 MPa was introduced into the chamber at a temperature of 35 °C, and the system was allowed to equilibrate for 1 h. Pressure in the chamber was held constant using two ISCO pumps running in constant pressure mode, and the pressure was measured using a digital pressure transducer (Omega) just below the chamber outlet. The temperature in the chamber was held constant using a surrounding air bath and a heat exchanger to warm the compressed CO_2. Every hour, the pressure was raised 0.5 MPa up to a maximum pressure of 9.5 MPa, which is just beyond our CAPP process operating conditions. The 1 h increments are consistent with the work published by Berens and Huvard,[49] suggesting that 1 h is adequate time for the CO_2 to equilibrate within the sample. As pressure increases, the solubility of CO_2 in the polymer samples increases, which plasticizes the tensile polymer samples and can lead to deformation. The samples were carefully observed for changes in size, shape, color, and morphology, and the sample length was measured after depressurization.

Results and Discussion

Size, Morphology, and Cross-Linking of Particles. The CAPP spraying process provides intimate mixing of the monomer/initiator/solvent solution and CO_2. These mixing conditions, coupled with the anti-solvent properties of the CO_2 (high diffusivity, low viscosity, high density, and high capacity for solvent extraction), facilitate the extraction of solvent from the sprayed solution, presumably leaving microdroplets containing mostly monomer and initiator. Illumination of these droplets of highly concentrated monomer and initiator with a high-powered light source results in rapid polymerization, subsequently followed by precipitation of cross-linked particles.

Figure 2 shows scanning electron micrographs of poly(PEG1KDA) microparticles formed using the CAPP process. The micrographs shown in Figure 2a−d illustrate the effects of varying the initiator concentrations from 1 to 1.5 to 2 to 4 wt % DMPA, respectively, while all other process conditions were held constant. The 1.5 and 2 wt % initiator samples (Figure 2b,c) exhibit relatively smooth, spherical particles with diameters in the range 0.5−50 μm. In contrast, the samples processed with 1 and 4 wt % DMPA exhibit strikingly different morphologies. There are some spheri-

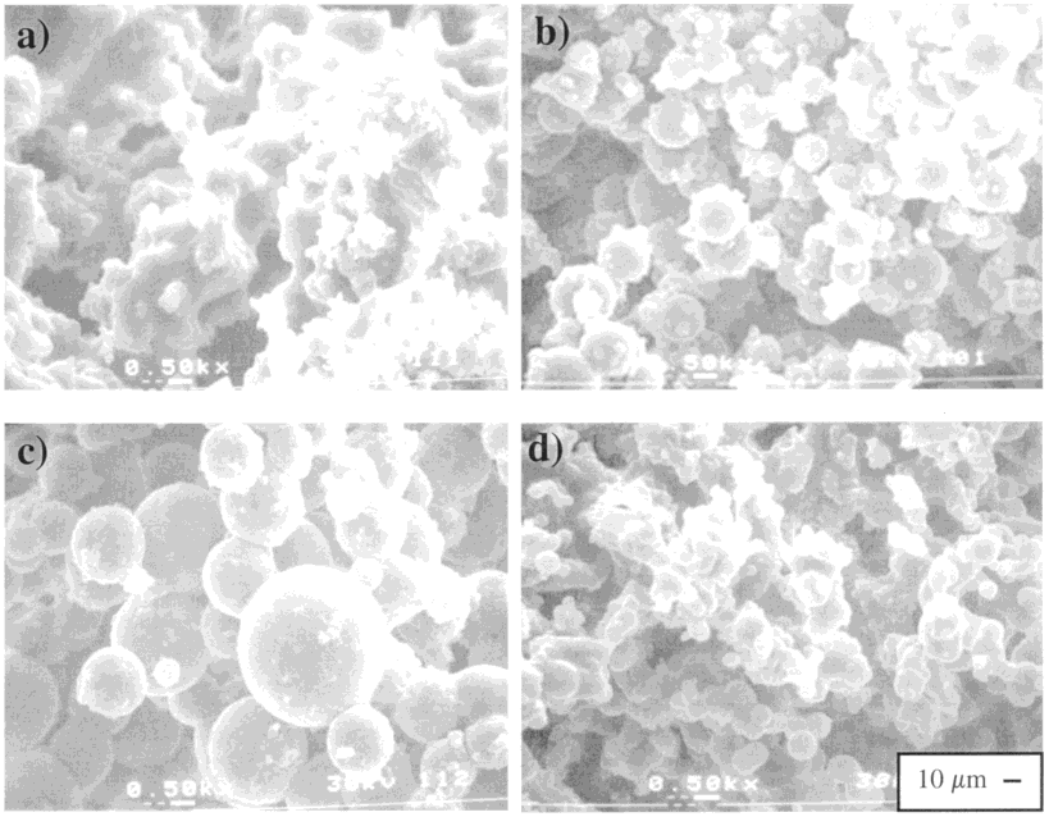

Figure 2. SEM photomicrographs of PEG 1000 particles processed in the CAPP system with various amounts of DMPA photoinitiator: (a) 1 wt %, (b) 1.5 wt %, (c) 2 wt %, and (d) 4 wt %.

cal particles in each micrograph, but the samples generally look like agglomerated particles with little uniformity in structure. These morphologies were reproducible when identical solutions were CAPP processed using equivalent operating conditions.

Since the rate of polymerization depends on the initiator concentration to the half power,[50,51] the time to reach a given conversion in the particles will increase with decreasing initiator concentration. In the case of the 1 wt % DMPA photoinitiator sample, the rate of polymerization was likely insufficient to produce significant conversion that would prevent particle agglomeration, and we therefore did not see the spherical structure as seen in other samples processed with higher photoinitiator concentrations. As for the samples processed with 4 wt % DMPA, too much initiator can lead to extremely high radical concentrations, elevated termination rates, and even primary radical termination, all of which can lead to decreased double-bond conversion.[52] Interestingly, the CAPP process shows a great deal of sensitivity to the initiation rate as evidenced with the resulting particle morphology even when the initiator concentration is changed only slightly. For example, the difference between 1 and 1.5 wt % DMPA corresponds to 20% difference in the rate of polymerization, yet the difference in particle morphology is dramatic.

Polymerization of the multifunctional PEG-based monomers during the CAPP particle processing was confirmed through FTIR spectroscopy of the particles compared to the monomer. Figure 3 shows conversion data for poly(PEG1KDA) microparticles produced at three different initiator concentrations and measured in triplicate. The particles from the experiments with varied amounts of initiator consistently reached conversions of about 75% or higher. These results are consistent with the SEM micrographs (Figure 2a,b) showing discrete particles and a spherical morphology for the 1.5 and 2 wt % photoinitiator samples, since the initiator concentration was great enough to sufficiently polymerize the particles before collision and agglomeration. Although the 1 wt % DMPA processed polymer particle samples reached a final conversion of greater than 75% (Figure 3), the polymerization rate was likely not great enough to form discrete particles in the short process residence time (about 2 min). No particles from the 4 wt % DMPA experiments were examined with respect to conversion because no particles were available for collection from the filter.

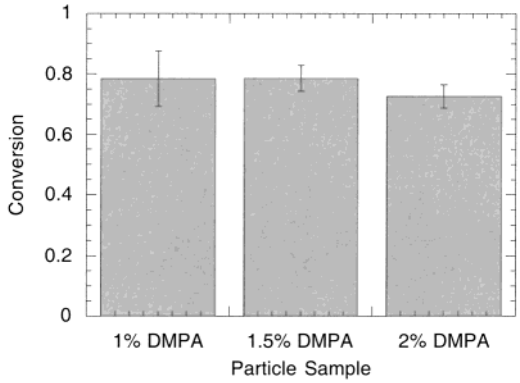

Figure 3. Average conversions of PEG1KDA monomer processed in the CAPP system with 2, 1.5, and 1 wt % DMPA to form particles. Conversions quantified using FTIR with peak area analysis.

The effect of varying light intensity on particle size and morphology in the CAPP system was also examined. Average incident light intensities of 6, 4, and 3 W/cm^2

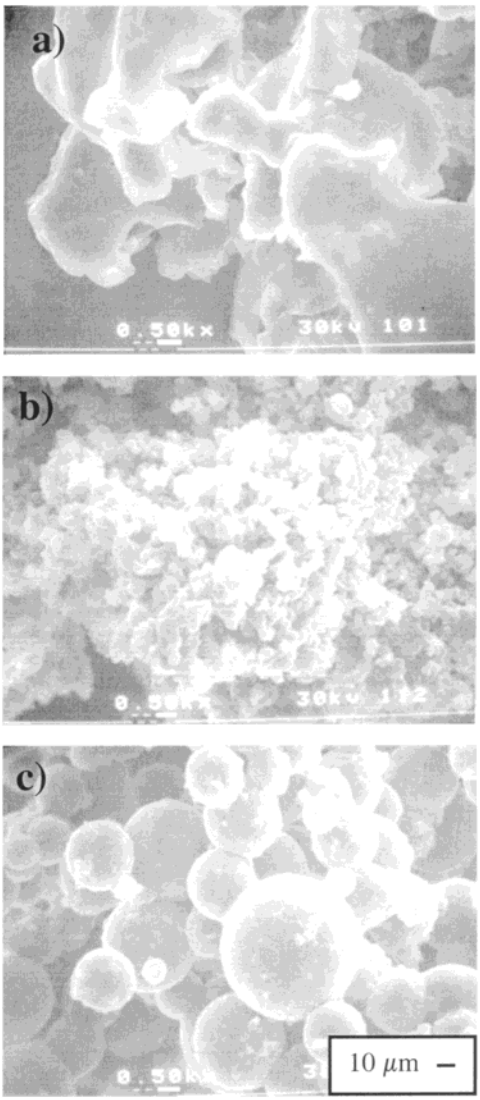

Figure 4. SEM photomicrographs of PEG 1000 particles processed in the CAPP system with various amounts average incident light intensity for the low, medium, and high runs, respectively: (a) 3, (b) 4, and (c) 6 W/cm^2.

(measured using the EFOS Novacure radiometer) were used for the high, medium, and low intensities, respectively, in conjunction with the CAPP process, and particles were collected and examined using SEM. For photoinitiated free radical polymerizations, the rate of polymerization typically depends on light intensity to the $^1/_2$ power. Unfortunately, it is hard to quantify the exact light intensity in the CAPP process as light is attenuated across the 3 cm thick chamber. In addition, the light is likely scattered and dispersed nonuniformly by the polymerizing particles located throughout the reaction chamber. Figure 4 shows samples from the low, medium, and high light intensity runs. Samples prepared at the low light intensity (Figure 4a) show little to no structure, judging from the large agglomerated masses and minimal evidence of particle formation. The most likely cause of this particle agglomeration is the reduced rate of initiation at a lower light intensity, and therefore a decreased rate of polymerization, permitting agglomeration before the particles gel. The medium-intensity experiment shown in Figure 4b exhibits an increased amount of particle formation but still significant numbers of agglomerates. Figure 4c shows nicely

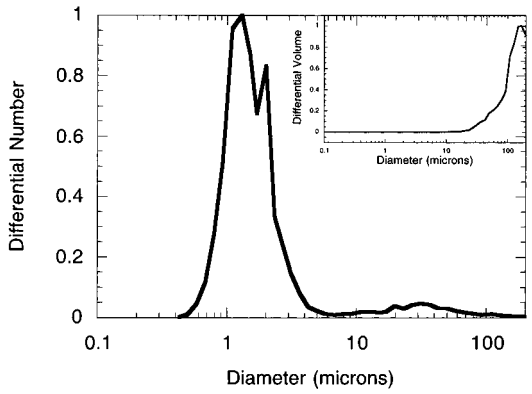

Figure 5. Particle size distribution for PEG 1000 particles processed in the CAPP system with 2 wt % DMPA. The solid line represents the geometric diameter size distribution. The dashed line represents the volumetric diameter size distribution.

formed spheres in size ranges from 1 to 50 μm. Consistent with the studies with varying initiator concentration, these results suggest that a higher initiation rate is more effective in producing cross-linked spherical particles in the limited time that the particles have to polymerize before they will interact with other particles in the high-pressure chamber due to the fluid mixing that occurs in the CAPP process.

Interestingly, it appears that small changes in both the incident light intensity and the initiator concentration have great effects on the resulting morphology of the particles formed in the CAPP process. As evidenced by the SEM micrographs, the CAPP process requires a specific minimum initiation rate to lock in the spherical particle morphology during the relatively short process residence time. It is curious that such small changes in each of these variables drastically affect the resulting morphology (we have observed similar results with other monomer systems) since the rate of polymerization is a relatively weak function of both the light intensity and initiator concentration; further studies are required to explore this behavior.

In addition to examining reaction conditions that enable particle formation, we were also interested in the size distribution of particles formed with the CAPP process. Figure 5 shows the particle size distribution for PEG1KDA polymerized at the high light intensity and with 2 wt % DMPA. The distribution of the geometric particle size was bimodal with a large number of particles with diameters between 1 and 3 μm and another significant population between 20 and 200 μm sized particles. Although SEM photomicrographs show only few particles, the particles examined with SEM exhibited diameters consistent with the samples measured using the Aerosizer, with a statistically significant number of particles counted. The volumetric distribution of particles illustrates that the total volume of particles is weighted, of course, heavily toward the particles with larger diameters, despite the fact that there are a greater number of smaller particles. The bimodal particle size distribution suggests two different mechanisms of particle formation. We hypothesize that the particle formation is a result of polymerization in both the liquid and gas phases of the system. We suspect that some of the monomer and initiator, facilitated by the solvent, dissolves into the SC-CO_2 phase, and the rest resides in sprayed droplets. When initiated, particles form from nucleation, growth, and polymerization processes in the

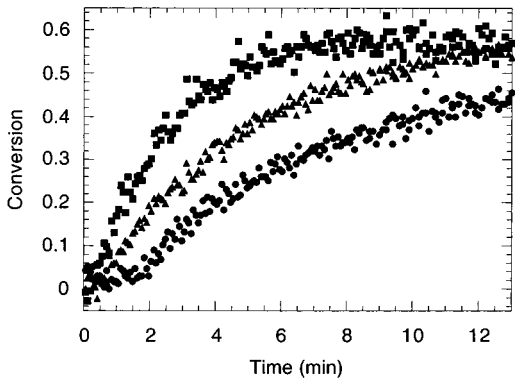

Figure 6. Conversion vs time data for PEG1KDA monomer in MC with 2 wt % DMPA polymerized using light intensities of (●) 1, (▲) 10, and (■) 20 mW/cm^2.

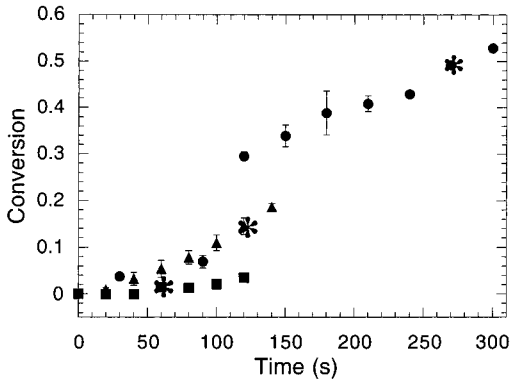

Figure 7. Conversion as a function of polymerization time for (■) 40, (▲) 25, and (●) 15 wt % PEG1KDA and 2 wt % DMPA in methylene chloride. The gel points of each solution are noted by the starred data points.

gas phase and strictly polymerization in the liquid droplets which would result in particles with the observed bimodal particle size distribution. Further studies are necessary to confirm this hypothesis and are underway. The relatively narrow size distribution (for the particles below 10 μm, the polydispersity = 2.9) observed, although bimodal, is important as these particles may be useful for drug delivery systems as previously mentioned.

Kinetic Studies. Multifunctional PEGDA monomers were chosen for the CAPP process because of their biocompatibility, their ability to form a highly cross-linked network, and the rapid reaction rate of acrylate groups. Furthermore, these monomers can be modified to make them biodegradable[43,53] through the addition of degradable lactic acid units. FTIR was used to examine the polymerization behavior of the PEG1KDA monomer as a function of light intensity and monomer concentration because these variables are readily controlled in the CAPP process. Figure 6 shows the double-bond conversion as a function of time for triplicate runs of 50% PEG1KDA in dry methylene chloride and light intensities of 1, 10, and 20 mW/cm^2. The resulting curves are typical of the behavior of multifunctional monomers where there is a short initial lag time as oxygen is likely scavenging radicals, followed by a rapid increase in conversion as autoacceleration takes place, followed by a plateau in the conversion where autodeceleration occurs and the reaction becomes diffusion limited. Conversion increases as a function of time for all three samples, but the initial slope, corresponding to the initial rate of polymerization, is greater for higher light intensities as expected. The high light intensity curve reaches a conversion of 55% in about 7 min, while the samples subjected to half the intensity require about 13 min to reach the same conversion. The samples polymerized with 1 mW/cm^2 light intensity only reached about 42% conversion in 13 min. Analysis of the conversion vs time curves (Figure 6) resulted in a dependence of the rate of polymerization on intensity to the 0.3−0.4 power, which is less than the theoretically expected value. Similar dependences on the rate of initiation, which is proportional to the light intensity, were observed in similar multifunctional monomer systems.[54] None of the samples reached 100% conversion, presumably due to the limited mobility of the reactive groups within the samples that occurs after autodeceleration causing trapped radicals, shielding of unreacted pendant groups, and isolated pools of unreacted monomer.[47,50]

When processing linear polymers using PCA, the temperature must be maintained below the operative T_g to obtain discrete particles. Analogously, for cross-linked polymers, the polymerization must proceed to a critical conversion, reaching the gel point, to preserve discrete particles. The gel point conversion can be adjusted by changing the concentration of monomer in the starting solution. As the concentration of monomer in the starting sample is increased, a lower conversion is necessary for gelation to occur. This trend is predictable as higher concentrations of monomer lead to an increased rate of polymerization ($R_p \sim$ [M]) and consequently increased cross-linked network formation for a given fractional conversion. Figure 7 shows the conversion as a function of time for 40, 25, and 15 wt % PEG1KDA in methylene chloride illuminated with 10 mW/cm^2 of 365 nm ultraviolet light with the experimentally observed gel point conversions of each solution noted by the starred data point. This effect works in favor of the CAPP process for particle formation by rapidly concentrating the monomer and thereby lowering the gel point conversion. We anticipate that in the CAPP process CO_2 will serve to rapidly remove solvent from the sprayed solutions, thereby increasing monomer concentrations and concomitantly increasing reaction rates and decreasing gel point conversions.

Mechanical Creep Studies. Mechanical creep experiments were performed on samples of PEG1KDA polymerized to various conversions ranging from 20 to 95%. None of the samples failed structurally, so changes in sample length and appearance were recorded. Figure 8 shows the maximum sample strain as a function of conversion for the samples subjected to the mechanical creep conditions described previously. As expected, samples with higher conversions experienced less deformation than those with lower conversions. Also, the samples at 20 and 55% conversion visually appeared moist in CO_2 at all pressures studied. Perhaps not surprisingly, discrete particles formed in the CAPP process all exhibited conversions greater than 75%.

This creep behavior can be related to the previous creep compliance studies with linear polymers[55−57] where it was discovered that polymer samples are severely plasticized by CO_2, which causes a considerable depression of the T_g. The T_g depression is significantly intensified when the CO_2 reaches the supercritical pressure and temperature, where the CO_2 exhibits the viscous properties of a gas but the density properties of a liquid. This T_g depression precludes many polymers

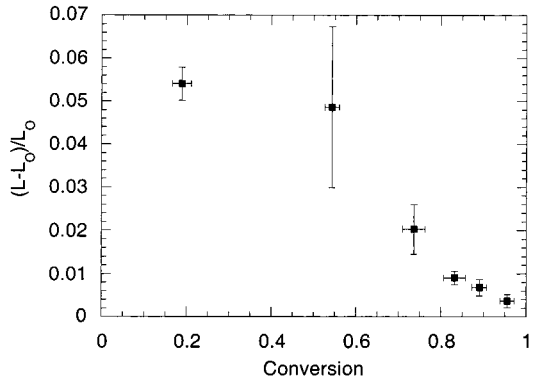

Figure 8. Normalized length of sample as a function of conversion for the samples subjected pressurized CO_2 in the mechanical creep experiments.

from processing in PCA style particle production methods due to the fact that they will not maintain their physical structure when introduced into a pressurized CO_2 environment.

Although we did observe some elongation of the tensile samples, the samples generally maintained their physical properties and structural integrity. Furthermore, it should be noted that as the conversion increased, the sample strain, and therefore the plasticization of the sample, lessened. This exemplifies one of the major benefits of this new CAPP process: T_g no longer limits the polymers (macromers and monomers) that can be processed in a compressed antisolvent, such as supercritical CO_2, since both the rate of polymerization and the resulting fractional conversion can be controlled to yield solid, spherical, cross-linked particles.

Conclusions

We have demonstrated a novel process for polymerizing polymer microparticles in situ during compressed antisolvent precipitation and explored with mechanical creep, gel point, and polymerization rate studies the conditions that are necessary for particle formation. Photopolymerization occurs when homogeneous solutions of monomer, initiator, and solvent are exposed to initiating light while being simultaneously sprayed into a compressed antisolvent. Using multifunctional monomers, the polymerization results in highly cross-linked microparticles with a consistent spherical morphology and a bimodal size distribution between 0.5 and 200 μm. Depending upon the solvent flow rate, the monomer type and functionality, the reactive group concentration, the initiation rate, and the operating conditions, various particle morphologies should be achievable.

Acknowledgment. This work was supported in part by grants from The Packard Foundation and NIH. J.L.O. gratefully acknowledges the National Science Foundation for a Graduate Research Fellowship.

References and Notes

(1) Brannon-Peppas, L. *Int. J. Pharm.* **1995**, *116*, 1−9.
(2) Nelson, C. L.; Hickmon, S. G.; Harrison, B. H. *Orthopedics* **1994**, *17*, 415−416.
(3) Wahlig, H.; Dingeldein, E.; Bergmann, R.; Reuss, K. *J. Bone Joint Surg.* **1978**, *60*, 270−275.
(4) Wiedmann, T. S.; DeCastro, L.; Wood, R. W. *Pharm. Res.* **1997**, *14*, 112−116.
(5) Edwards, D.; Hanes, J.; Caponetti, G.; Hrkach, J.; BenJebria, A.; Eskew, M.; Mintzes, J.; Deaver, D.; Lotan, N.; Langer, R. *Science* **1997**, *276*, 1868−1871.
(6) Mathiowitz, E.; Langer, R. *J. Controlled Release* **1987**, *5*, 13−22.
(7) Sanchez, A.; Gupta, R. K.; Alonso, M. J.; Siber, G. R.; Langer, R. *J. Pharm. Sci.* **1996**, *85*, 547−552.
(8) Wheatley, M.; Langer, R. *Part. Sci. Technol.* **1987**, *5*, 53−64.
(9) Herbert, P.; Murphy, K.; Johnson, O.; Dong, N.; Jaworowicz, W.; Tracy, M. A.; Cleland, J. L.; Putney, S. D. *Pharm. Res.* **1998**, *15*, 357−361.
(10) Park, T. G.; Alonso, M. J.; Langer, R. *J. Appl. Polym. Sci.* **1994**, *52*.
(11) Soriano, I.; Delgado, A.; Diaz, R. V.; Evora, C. *Drug Dev. Ind. Pharm.* **1995**, *21*, 549−558.
(12) Lu, W. Q.; Park, T. G. *Biotechnol. Prog.* **1995**, *11*, 224−227.
(13) Tabata, Y.; Ikada, Y. *Pharm. Res.* **1989**, *6*, 422−427.
(14) Heya, T.; Okada, H.; Ogawa, Y.; Toguchi, H. *J. Pharm. Sci.* **1994**, *83*, 636−640.
(15) Hora, M. S.; Rana, R. K.; Nunberg, J. H.; Tice, T. R.; Gilley, R. M.; Hudson, M. E. *Pharm. Res.* **1990**, *7*, 1190−1194.
(16) Niwa, T.; Takeuchi, H.; Hino, T.; Kunou, N.; Kawashimi, Y. *J. Pharm. Sci.* **1994**, *83*, 727−732.
(17) Cheng, C. M.; Vanderhoff, J. W.; El-Aasser, M. S. *J. Polym. Sci., Part A: Polym. Chem.* **1992**, *30*, 245−56.
(18) Cleek, R.; Ting, K.; Eskin, S.; Mikos, A. *J. Controlled Release* **1997**, *48*, 259−268.
(19) Huang, Y.; Chung, T.; Tzeng, T. *Int. J. Pharm.* **1997**, *156*, 9−15.
(20) Kriwet, B.; Walter, E.; Kissel, T. *J. Controlled Release* **1998**, *56*, 149−158.
(21) Yang, Y.; Chung, T.; Ng, N. *Biomaterials* **2000**, *22*, 231−241.
(22) Canelas, D.; DeSimone, J. *Adv. Polym. Sci.* **1997**, *133*, 103−140.
(23) Tom, J.; Debenedetti, P. *J. Aerosol Sci.* **1991**, *22*, 555−584.
(24) Tom, J. W.; Debenedetti, P. G. *Biotechnol. Prog.* **1991**, *7*, 403−411.
(25) McHugh, M.; Krukonis, V. *Supercritical Fluid Extraction*; Butterworth-Heineman: Woburn, MA, 1994.
(26) Bodmeier, R.; Wang, H.; Dixon, D. J.; Mawson, S.; Johnston, K. P. *Pharm. Res.* **1995**, *12*, 1211−1217.
(27) Dixon, D. J.; Johnston, K. P. *J. Appl. Polym. Sci.* **1993**, *50*, 1929−1942.
(28) Dixon, D. J.; Lunabarcenas, G.; Johnston, K. P. *Polymer* **1994**, *35*, 3998−4005.
(29) Randolph, T. W.; Randolph, A. D.; Mebes, M.; Yeung, S. *Biotechnol. Prog.* **1993**, *9*, 429−435.
(30) Connon, C.; Falk, R.; Randolph, T. *Macromolecules* **1999**, *32*, 1890−1896.
(31) DeSimone, J. M.; Guan, Z.; Elsbernd, C. S. *Science* **1992**, *257*, 945−947.
(32) Guan, Z. B.; Combes, J. R.; Menceloglu, Y. Z.; Desimone, J. M. *Macromolecules* **1993**, *26*, 2663−2669.
(33) Combes, J. R.; Guan, Z.; Desimone, J. M. *Macromolecules* **1994**, *27*, 865−867.
(34) Shiho, H.; DeSimone, J. *J. Polym. Sci., Part A: Polym. Chem.* **1999**, *37*, 2429−2437.
(35) Romack, T. J.; Maury, E. E.; Desimone, J. M. *Macromolecules* **1995**, *28*, 912−915.
(36) DeSimone, J. M.; Maury, E. E.; Menceloglu, Y. Z.; McClain, J. B.; Romack, T. J.; Combes, J. R. *Science* **1994**, *5170*, 356−359.
(37) Hsiao, Y. L.; Maury, E. E.; Desimone, J. M.; Mawson, S.; Johnston, K. P. *Macromolecules* **1995**, *28*, 8159−8166.
(38) Canelas, D.; Betts, D.; DeSimone, J.; Yates, M.; Johnston, K. *Macromolecules* **1998**, *31*, 6794−6805.
(39) Vorderbruggen, M. A.; Wu, K.; Breneman, C. M. *Chem. Mater.* **1996**, *8*, 1106−11.
(40) Esen, C.; Schweiger, G. *J. Colloid Interface Sci.* **1996**, *179*, 276−80.
(41) Anseth, K.; Svaldi, D.; Laurencin, C.; Langer, R. *ACS Symp. Ser.* **1997**, *673*, 189−202.
(42) Mason, M. N.; Metters, A. T.; Bowman, C. N.; Anseth, K. S. *Macromolecules* **2001**, *34*, 4630−4635.
(43) Sawhney, A.; Pathak, C.; Hubbell, J. *Macromolecules* **1993**, *26*, 581−587.
(44) Falk, R.; Randolph, T. W.; Meyer, J. D.; Kelly, R. M.; Manning, M. C. *J. Controlled Release* **1997**, *44*, 77−85.
(45) Bleich, J.; Muller, B. W.; Wassmus, W. *Int. J. Pharm.* **1993**, *97*, 111−117.
(46) Fischer, W.; Muller, B. W. Method and apparatus for the manufacture of a product having a substance embedded in a carrier. US Patent #5043280, 1991.
(47) Lovell, L. G.; Berchtold, K. A.; Elliott, J. E.; Lu, H.; Bowman, C. N. *Polym. Adv. Technol.* **2001**, *12*, 335−345.

(48) Decker, C. *J. Polym. Sci., Part A: Polym. Chem.* **1992**, *30*, 913−928.
(49) Berens, A.; Huvard, G. *ACS Symp. Ser.* **1989**, *406*, 207−223.
(50) Kloosterboer, J. *Adv. Polym. Sci.* **1988**, *84*, 1−61.
(51) Odian, G. *Principles of Polymerization*, 3rd ed.; John Wiley & Sons: New York, 1991.
(52) Kloosterboer, J. G.; Lijten, G. F. C. M.; GreiDanus, F. J. A. M. *Polym. Commun.* **1986**, *27*, 268−271.
(53) Metters, A.; Anseth, K.; Bowman, C. *Polymer* **2000**, *41*, 3993−4004.
(54) Berchtold, K.; Lovell, L.; Nie, J.; Hacioglu, B.; Bowman, C. *Polymer* **2001**, *42*, 4925−4929.
(55) Condo, P. D.; Sanchez, I. C.; Panayiotou, C. G.; Johnston, K. P. *Macromolecules* **1992**, *25*, 6119−6127.
(56) Condo, P. D.; Paul, D. R.; Johnston, K. P. *Macromolecules* **1994**, *27*, 365−371.
(57) Condo, P. D.; Johnston, K. P. *J. Polym. Sci., Part B: Polym. Phys.* **1994**, *32*, 523−533.

MA011955K